Glutathione adducts induced by ischemia and deletion of glutaredoxin-1 stabilize HIF-1α and improve limb revascularization

Yosuke Watanabe[a,b], Colin E. Murdoch[a,b,1], Soichi Sano[b], Yasuo Ido[c], Markus M. Bachschmid[a,b], Richard A. Cohen[a,b], and Reiko Matsui[a,b,2]

[a]Vascular Biology Section, Boston University School of Medicine, Boston, MA 20118; [b]Whitaker Cardiovascular Institute, Boston University School of Medicine, Boston, MA 20118; and [c]Section of Endocrinology, Boston University School of Medicine, Boston, MA 20118

Edited by Gregg L. Semenza, Johns Hopkins University School of Medicine, Baltimore, MD, and approved April 15, 2016 (received for review December 14, 2015)

Reactive oxygen species (ROS) are increased in ischemic tissues and necessary for revascularization; however, the mechanism remains unclear. Exposure of cysteine residues to ROS in the presence of glutathione (GSH) generates GSH-protein adducts that are specifically reversed by the cytosolic thioltransferase, glutaredoxin-1 (Glrx). Here, we show that a key angiogenic transcriptional factor hypoxia-inducible factor (HIF)-1α is stabilized by GSH adducts, and the genetic deletion of Glrx improves ischemic revascularization. In mouse muscle C2C12 cells, HIF-1α protein levels are increased by increasing GSH adducts with cell-permeable oxidized GSH (GSSG-ethyl ester) or 2-acetylamino-3-[4-(2-acetylamino-2-carboxyethylsulfanyl thiocarbonylamino) phenylthiocarbamoylsulfanyl] propionic acid (2-AAPA), an inhibitor of glutathione reductase. A biotin switch assay shows that GSSG-ester-induced HIF-1α contains reversibly modified thiols, and MS confirms GSH adducts on Cys^{520} (mouse Cys^{533}). In addition, an HIF-1α Cys^{520} serine mutant is resistant to 2-AAPA–induced HIF-1α stabilization. Furthermore, Glrx overexpression prevents HIF-1α stabilization, whereas Glrx ablation by siRNA increases HIF-1α protein and expression of downstream angiogenic genes. Blood flow recovery after femoral artery ligation is significantly improved in *Glrx* KO mice, associated with increased levels of GSH-protein adducts, capillary density, vascular endothelial growth factor (VEGF)-A, and HIF-1α in the ischemic muscles. Therefore, Glrx ablation stabilizes HIF-1α by increasing GSH adducts on Cys^{520} promoting in vivo HIF-1α stabilization, VEGF-A production, and revascularization in the ischemic muscles.

GSH-protein adducts | *S*-glutathionylation | hypoxia-inducible factor-1 | glutaredoxin-1 | ischemic limb revascularization

Despite the notion that increased oxidants are deleterious, clinical trials of antioxidant therapies failed to prevent cardiovascular diseases (1). In mouse models, decreasing reactive oxygen species (ROS) impaired ischemic revascularization after hind limb ischemia (2, 3), and in contrast, increased ROS (4) or decreased antioxidants (5) improved ischemic revascularization. Therefore, ROS play a protective role in ischemic revascularization. However, little is known about the molecular mechanism by which ROS improve ischemic revascularization.

It is generally recognized that ROS change protein function by posttranslational modifications of cysteine thiols (-SH) (6). Protein thiols are susceptible to oxidation and give rise to reversible oxidative modifications including *S*-sulfenylation (-SOH), *S*-nitrosylation (-SNO), and glutathione (GSH)-protein adducts [*S*-glutathionylation (-SSG)] (7). These reversible modifications can regulate cellular signaling and may contribute to ROS-induced ischemic revascularization. Interestingly, *S*-nitrosylation has been indicated as a mechanism of nitric oxide (NO)-mediated signaling and shown to stabilize hypoxia-inducible factor (HIF)-1α, a master angiogenic transcriptional regulator (8).

S-nitrosylation and *S*-sulfenylation are chemically unstable and further react with GSH, which is the most abundant small intracellular thiol, to form GSH adducts (9, 10). A cytosolic thioltransferase, glutaredoxin-1 (Glrx), specifically and efficiently catalyzes reduction of GSH-protein adducts (11); thus, Glrx-regulated GSH-protein adducts can affect redox signaling and play an important role in pathophysiological conditions (12). The role of GSH-protein adducts of potential in vivo target proteins in ischemic revascularization has not been elucidated. We showed that Glrx overexpression impairs mouse ischemic revascularization (13). Here we hypothesized that GSH-protein adducts may prevent degradation of HIF-1α and that Glrx might control HIF-1α activity by reversing GSH adducts. We demonstrate that HIF-1α is stabilized by GSH adducts on Cys^{520} as a consequence of ischemia or depletion of Glrx. Consistent with this, *Glrx* KO mice have improved ischemic limb revascularization.

Results

Effect of GSH Adducts on HIF-1α Stabilization. To specifically increase GSH-protein adducts in vitro, the cell membrane permeable oxidized glutathione (GSSG)-ethyl ester (GSSG-EE) was used (9). C2C12 cells treated for 10 h with GSSG-EE exhibited increased levels of HIF-1α (Fig. 1*A*). Similarly, an inhibitor of glutathione reductase, 2-acetylamino-3-[4-(2-acetylamino-2-carboxyethylsulfanyl thiocarbonylamino) phenylthiocarbamoylsulfanyl] propionic acid (2-AAPA), which increases GSH-protein adducts (14), increased HIF-1α protein levels (Fig. S1). These data indicate that increased GSH-protein adducts increase HIF-1α stabilization. A biotin switch assay was performed to detect reversible oxidative thiol modification of

Significance

Glutathione (GSH)-protein adducts are oxidative posttranslational modifications that are reversed by glutaredoxin-1 (Glrx). We show that ischemia-induced oxidants promote revascularization through GSH adducts on hypoxia-inducible factor (HIF)-1α, an angiogenic transcriptional factor. GSH adducts on Cys^{520} stabilize HIF-1α protein, and depletion of Glrx stabilizes HIF-1α in vitro and increases angiogenic gene expression. Glrx ablation in vivo increases GSH adducts in ischemic muscles after femoral artery ligation in mice and improves blood flow recovery associated with increased HIF-1α and VEGF expression. Thus, increased GSH-protein adducts on HIF-1α in ischemic limbs are beneficial in promoting angiogenesis. Our data indicate HIF-1α is a novel in vivo target of Glrx, and inhibition of Glrx is a potential therapeutic strategy to improve ischemic limb revascularization.

Author contributions: Y.W., C.E.M., and R.M. designed research; Y.W. performed research; C.E.M., S.S., and Y.I. contributed new reagents/analytic tools; Y.W., M.M.B., and R.M. analyzed data; and Y.W., R.A.C., and R.M. wrote the paper.

The authors declare no conflict of interest.

This article is a PNAS Direct Submission.

[1]Present address: Aston Medical Research Institute, Aston Medical School, Aston University, Birmingham B47ET, United Kingdom.

[2]To whom correspondence should be addressed. Email: rmatsui@bu.edu.

This article contains supporting information online at www.pnas.org/lookup/suppl/doi:10.1073/pnas.1524198113/-/DCSupplemental.

HIF-1α. In this assay, modified cysteine thiols were reduced and stably labeled with biotin-iodoacetamide (BIAM) followed by pull-down using streptavidin beads as previously described (15). GSSG-EE treatment increased overall levels of biotin-labeled proteins in cell lysates of C2C12 cells (Fig. 1*B*) and confirmed that GSSG-EE–treated cells contained higher levels of reversible modified proteins than vehicle-treated cells. HIF-1α was detected in the pulled-down proteins, indicating that HIF-1α had reversible thiol modifications augmented by GSSG-EE treatment (Fig. 1*B*).

To identify GSH-protein adducts of specific cysteine residues of HIF-1α, MS was performed on recombinant human HIF-1α treated with a mixture of GSSG/GSH. LC/MS/MS analysis showed that among 15 cysteines in human HIF-1α, only 2 cysteine residues were modified with GSH adduct and one of them was Cys^{520} (Fig. 1*C*). This cysteine residue is conserved widely in vertebrate species and is the only cysteine residue in the oxidant-dependent degradation domain (ODD) of human HIF-1α (8). GSH-protein adducts do not always affect protein function (12). To investigate the role of the GSH adduct of Cys^{520}, a Cys^{520}→Ser mutant HIF-1α was generated. First, endogenous HIF-1α was knocked down by the CRISPR/Cas9 system. Decreased protein levels of HIF-1α were confirmed after induction by $CoCl_2$ (Fig. S2*A*). Reconstitution of HIF-1α in COS7 cells was performed by transfecting plasmids encoding WT or C520S mutant HIF-1α to COS7 cells depleted of HIF-1α. Two days after the transfection, 2-AAPA was used to induce GSH adduct-dependent HIF-1α stabilization. Treatment with 2-AAPA increased HIF-1α expression in WT HIF-1α, but not in Cys^{520} HIF-1α mutant-transfected cells (Fig. 1 *D* and *E*). In normoxia, HIF-1α is hydroxylated by oxygen-dependent prolyl hydroxylase, and hydroxylated HIF-1α is ubiquitinated by attachment of the E3 ubiquitin ligase, von Hippel–Lindau tumor suppressor protein (pVHL), to the ODD leading to proteasomal degradation (16, 17). To elucidate the mechanism of HIF-1α stabilization, we tested whether pVHL attachment to HIF-1α is decreased by GSH adduct on Cys^{520} located in the ODD. To examine this protein interaction, cell lysate of HEK293T cells expressing Flag-tagged WT or C520S mutant HIF-1α was treated with GSSG to increase GSH adducts on HIF-1α, and then coimmunoprecipitation (Co-IP) was performed with cell lysates containing HA-pVHL. As expected, pVHL attachment was decreased by GSSG treatment in WT but not in C520S mutant HIF-1α cell lysates (Fig. 1*F*). Expression and hydroxylation levels of HIF-1α were not different in WT or C520S mutant HIF-1α–expressing cells (Fig. S3).

Regulation of HIF-1α and Angiogenic Genes by Glrx. The levels of protein-GSH adducts are specifically regulated by gain and loss of function of Glrx (13, 18). To analyze the effect of removal of GSH adducts by Glrx on HIF-1α stabilization, Glrx was overexpressed in COS-7 cells using adenoviral tetracycline-responsive element–driven Glrx (Ad tet-Glrx) (19), and doxycycline was added to induce Glrx in Ad tet-Glrx–transfected cells. Glrx overexpression decreased accumulation of HIF-1α induced by 2-AAPA (Fig. 2 *A* and *B*). Also, the effect of Glrx ablation was analyzed by adding siRNA to mouse Glrx (siGlrx) in C2C12 cells. Glrx protein was almost completely knocked down in C2C12 cells by siGlrx (Fig. 2*C*). HIF-1α was significantly increased in cells treated with siGlrx compared with control siRNA (Fig. 2 *C* and *D*). The biotin switch assay confirmed that siGlrx-treated cells contained higher levels of proteins with reversibly oxidized thiols including HIF-1α, indicating that HIF-1α had reversible thiol modifications augmented by Glrx inhibition (Fig. S4). Although HIF-1α protein was increased, Glrx ablation did not affect mRNA levels of HIF-1α (Fig. 2*E*), indicating that HIF-1α was regulated at the protein level. Furthermore, in siGlrx-treated cells, mRNA expression of HIF-1α–dependent angiogenic genes was increased compared with control including Vegfa, Pdgf (platelet-derived growth factor) a, Pdgfb, and Fgf (fibroblast growth factor) 2 (Fig. 2*F*), indicating that HIF-1α transcriptional activity was increased by siGlrx. Furthermore, the effect of Glrx knockdown on HIF-1α stabilization was eliminated by overexpression of human Glrx, which is resistant to mouse siGlrx (Fig. 2*G*). To confirm that the increase in angiogenic genes caused by Glrx knockdown depends on HIF-1α, Glrx knockdown by siRNA was performed to C2C12 cells in which the HIF-1α gene was knocked down by CRISPR/Cas9. Levels of HIF-1α in HIF-1α knockdown cells were 52% of that in control cells after $CoCl_2$ treatment (Fig. S2*B*). The increase in Vegfa mRNA expression caused by siGlrx was eliminated in cells with the HIF-1α knockdown (Fig. 2*H*).

Lack of Glrx Improves Ischemic Hind Limb Revascularization in Mice. GSH-protein adducts were increased in ischemic hind limbs; in contrast, GSH protein adducts were decreased in transgenic mice overexpressing Glrx, resulting in impaired revascularization (13). Here, to determine the role of endogenous Glrx on ischemic revascularization, hind limb ischemia was induced in *Glrx* KO and WT littermate controls. A mouse model of peripheral artery disease was created in 10- to 12-wk-old male mice by excising a 5-mm segment of left femoral artery. Blood flow was measured serially by using LASER (light amplification by stimulated emission of radiation) Döppler before, immediately after hind limb ischemic surgery, and at days 3, 7, and 14 (Fig. 3*A*). Notably, blood flow recovery after hind limb ischemia was significantly improved in *Glrx* KO mice compared with WT littermates (Fig. 3*B*). After 14 d, the blood flow in ischemic limbs returned to 91% of nonischemic limbs in *Glrx* KO mice, whereas it was still 70% in WT mice. In addition, histological analysis of ischemic limbs 7 d after surgery showed that necrotic areas, characterized by loss of muscle fibers and infiltration of inflammatory cells that appeared in WT mice, were less obvious in the ischemic limb of *Glrx* KO mice (Fig. 3*C*). Capillary density in nonischemic limbs was not different between *Glrx* KO mice and WT mice, but capillary density, which is increased in ischemic limbs of WT mice, was increased to a greater extent in *Glrx* KO mice (Fig. 3 *D* and *E*). To analyze GSH-protein adducts in ischemic limbs, an immunoblot using anti-GSH antibody was performed on muscle proteins under nonreducing conditions. The levels of GSH-protein adducts were not different in nonischemic limbs between *Glrx* KO and WT mice. Levels increased in ischemic limbs of both types of mice, but the increase was significantly greater in *Glrx* KO ischemic limbs (Fig. 3 *F* and *G*). Similarly, the levels of oxidatively modified proteins detected by the biotin switch assay were greater in *Glrx* KO ischemic limbs than WT ischemic limbs (Fig. S5). Increases in HIF-1α and VEGF-A in ischemic limbs were significantly greater in *Glrx* KO mice than in WT mice (Fig. 3 *H*–*J*).

To explore the roles of Glrx in myeloid cells in blood flow recovery, bone marrow from *Glrx* KO mice and WT littermates was transplanted to WT recipient mice. Expression of Glrx in bone marrow was eliminated, but not in limb muscle, after *Glrx* KO marrow transplantation (Fig. S6*A*). Interestingly, *Glrx* KO marrow transplantation had no effect on blood flow recovery after hind limb ischemia surgery (Fig. S6*B*), indicating that Glrx in resident tissue cells was more important in regulating blood flow recovery.

Discussion

GSH-protein adducts (*S*-glutathionylation) has emerged as an important oxidative thiol modification that regulates signaling molecules and transcription factors (6, 7, 9, 12). This modification is specifically reversed by Glrx, a ubiquitous cytosolic enzyme. Although many proteins are functionally regulated by GSH adducts (20–23), Glrx-mediated functional control in vivo is not shown for many molecules (24). The previously unidentified findings in this study are (*i*) that HIF-1α stability is regulated by glutathione adducts and by endogenous Glrx in vivo during ischemia, (*ii*) that glutathione adducts stabilize HIF-1α by preventing pVHL binding despite hydroxylation, and (*iii*) that endogenous Glrx significantly suppresses ischemic revascularization, making it a therapeutic target. This study provides one of the mechanisms that ROS stimulate ischemic revascularization and emphasizes caution in the use of antioxidants for ischemia.

HIF-1α is a key regulator of the response to hypoxia and is mediated by the HIF-1α subunit and the constitutively expressed HIF-1β subunit. Hypoxia inactivates prolyl hydroxylase and stabilizes HIF-1α by preventing protein degradation. HIF-1α is a major factor contributing to ischemic revascularization (25, 26). Interestingly, previous reports indicated NO-induced HIF-1α stabilization by

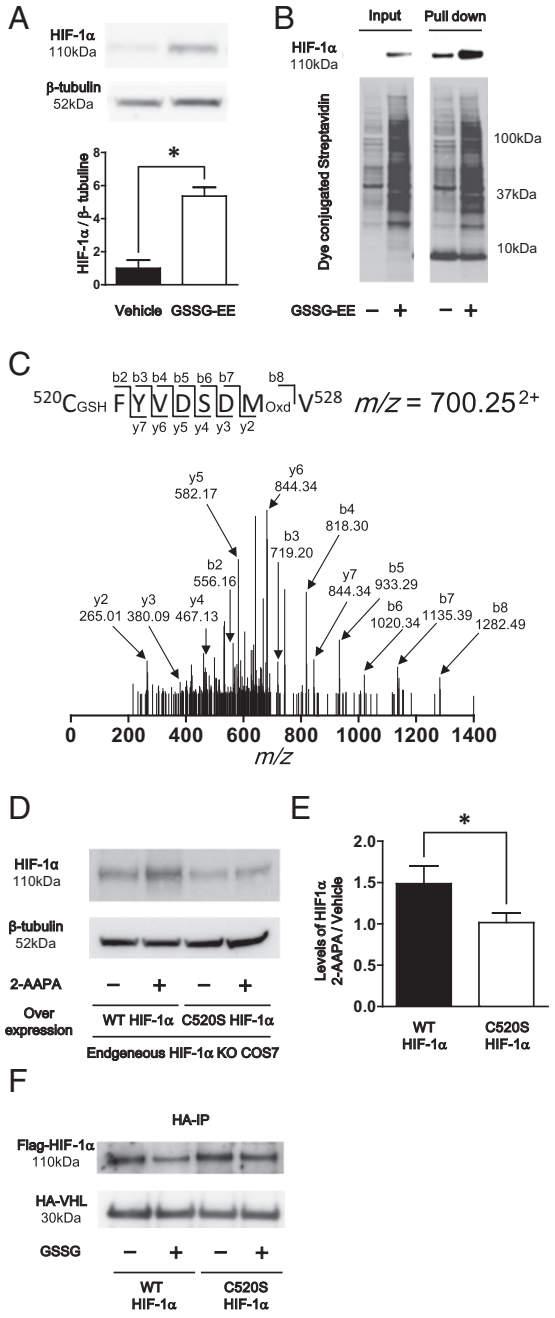

Fig. 1. Effect of GSH adduct on HIF-1α stabilization. (*A*) Effect of GSSG-ethyl-ester on HIF-1α stabilization in C2C12 cells. After differentiation, C2C12 cells were treated with 50 μg GSSG-ethyl ester or PBS for 10 h. Representative Western blot of HIF-1α and β-tubulin (*Upper*) and densitometry analysis of HIF-1α normalized by β-tubulin (*Lower*) (n = 8 each group). (*B*) Biotin switching assay for detection of HIF-1α reversible oxidative modification. DTT-dependent oxidative modified cysteines were labeled with biotin. Then biotin labeled protein was pull-downed using streptavidin beads. (*B*) Immunoblot of HIF-1α (*Upper Left*) and total reversible oxidative modified proteins detected by dye conjugated streptavidin (*Lower Left*) in a total sample. Immunoblot of HIF-1α (*Upper Right*) and total reversible oxidative modified proteins (*Lower Right*) in pulled down proteins. (*C*) Identification of Cys^{520} GSH adduct by MS. GSH adduct of Cys^{520} was detected from elastase fragment ^{520}CFYVDSDMV^{528}. The actual mass of this fragment was 1,939.48 ($m/z = 700.25^{2+}$), which was 321 Da more than the original MW. The MS/MS analysis showed that this fragment modified at Cys^{520} by GSH adduct (+305 Da) and Met^{527} by oxidation (+16 Da). (*D* and *E*) C520S mutation decreased 2-AAPA–dependent stabilization of HIF-1α. Plasmids that included WT and C520S mutant HIF-1α were transfected to COS7 cells in which endogenous HIF-1α was deleted by CRISPR/Cas9. These cells were treated with 20 μmol/L 2-AAPA for 3 h. (*D*) Representative Western blot of HIF-1α and β-tubulin. (*E*) Densitometry analysis, data were expressed as HIF-1α induction ratio of 2-AAPA–treated cells to respective vehicle-treated cells (n = 4 each group). (*F*) Western blotting analysis following Co IP of HA-VHL overexpressed cell lysate and GSSG-treated Flag-tagged WT or C520S mutant HIF-1α–overexpressed cell lysate by anti-HA antibody. Detection of Flag-tagged HIF-1α and HA-tagged VHL was performed by anti-Flag antibody and anti-VHL antibody, respectively. Experiments were repeated three times with similar results. *$P < 0.05$.

S-nitrosylation (27) and showed that Cys^{533} (equivalent to human Cys^{520}) in the ODD was critical for NO-induced dissociation of the ODD from pVHL to prevent HIF-1α degradation (8). We detected GSH adduct on Cys^{520} of human HIF-1α by MS, and by using a HIF-1α Cys^{520} Ser mutant, confirmed that GSH adducts on this cysteine are critical for preventing binding to pVHL and HIF-1α stabilization.

To distinguish *S*-nitrosylation from GSH-protein adducts in vivo is technically difficult because (*i*) reactive nitrogen species such as *S*-nitrosoglutathione (GSNO) or peroxynitrite ($ONOO^-$) can induce both *S*-nitrosylation and GSH-protein adducts (9, 28), (*ii*) *S*-nitrosylation is chemically unstable and can react with GSH to become relatively more stable GSH adducts (9, 10), and (*iii*) biotin switch assays are not very specific to distinguish these reversible modifications (29). In our study, HIF-1α stabilization was induced by GSSG-EE in C2C12 cells under conditions of minimal nitrosative stress, and its stabilization was regulated by Glrx, which specifically reverses GSH-protein adducts. Furthermore, Glrx deletion in vivo stabilized HIF-1α and promoted revascularization, but levels of S-nitrosylated proteins detected by an ascorbate-dependent biotin switch assay were not different either between ischemic and nonischemic limbs or between WT and *Glrx* KO limbs (Fig. S7). These data contrast with increased GSH adducts in ischemic muscles and further increases in the *Glrx* KO mouse shown by Western blot (Fig. 3*F*) and by data on DTT-reducible thiol adducts obtained with the biotin switch assay (Fig. S5). These results indicate a significant role of GSH adducts, rather than *S*-nitrosylation per se, in HIF-1α stabilization and ischemic angiogenesis.

The effects of ischemia in vivo are caused not only by hypoxia, but ROS are also produced by mitochondria, NADPH oxidases, and other sources (30). Previous studies indicated that ROS transduce angiogenic signaling and promote revascularization (4). Our data suggest that ROS promote ischemic revascularization at least in part by increasing GSH adducts on HIF-1α. Therefore, increased levels of GSH-protein adducts in ischemic muscle in WT mice may not merely be an indication of oxidative stress but rather are evidence of a pathophysiological response that facilitates revascularization.

Previously, we reported that Glrx-overexpressing transgenic (TG) mice had impaired ischemic limb revascularization in association with enhanced endothelial NF-κB activity and increased plasma levels of the antiangiogenic soluble VEGFR1 (sFlt1) (13). NF-κB may increase inflammation and sFlt1 induction, but endothelial NF-κB KO impaired blood flow recovery in ischemic hind limb (31). Therefore, although Glrx deletion may inactivate NF-κB by GSH-protein adducts on IKK-β (22) or p50 (23), NF-κB inactivation per se cannot explain improved blood flow in *Glrx* KO mice. Also, plasma sFlt1 levels were not different between *Glrx* KO and WT mice after hind limb ischemia (Fig. S8). Our interpretation is that superphysiological overexpression of Glrx induces sFlt1, but endogenous Glrx has little effect on sFlt1 expression. From our TG and KO mice studies, we can conclude that Glrx has antiangiogenic actions in vivo, but the mechanisms that explain the phenotypes are complex and may also include regulation of additional proteins by GSH adducts including sarcoendoplasmic reticulum calcium ATPase (21, 32) and tyrosine phosphatase PTP1B (20). However, the increase in VEGF-A expression induced by siGlrx was dependent on HIF-1α in C2C12 cells (Fig. 2*H*), indicating that HIF-1α is the major mediator of proangiogenic responses by Glrx ablation.

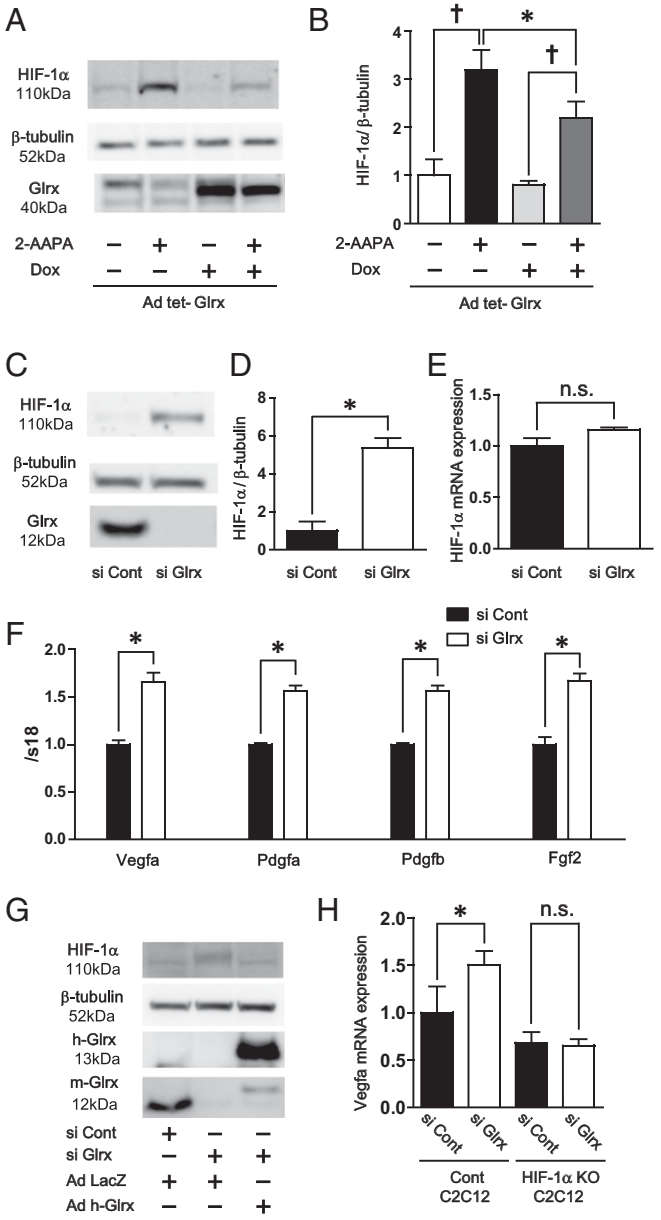

Fig. 2. Regulation of HIF-1α and angiogenic genes by Glrx. (*A* and *B*) Glrx overexpression decreased 2-AAPA–dependent HIF-1α stabilization. Ad tet-Glrx was transfected to COS7 cells. After Glrx overexpression was induced by 1 μg doxycycline, these cells were treated with 2-AAPA. (*A*) Representative Western blot of HIF-1α, β-tubulin, and Glrx. (*B*) Densitometry analysis of HIF-1α normalized by β-tubulin ($n = 4$ each group). Glrx knockdown increased HIF-1α and angiogenic genes expression. (*C* and *D*) Glrx knockdown by siGlrx increased HIF-1α and angiogenic genes in C2C12 cells. (*C*) Representative Western blot of HIF-1α, β-tubulin, and Glrx. (*D*) Densitometry analysis of HIF-1α ($n = 8$ each group). (*E*) Relative mRNA expression of HIF-1α, (*F*) mRNA of Vegfa, Pdgfa, Pdgfb, and Fgf2 ($n = 6$ each group) in siGlrx-treated C2C12 cells. (*G*) Overexpression of human Glrx effect on HIF-1α stabilization by Glrx knockdown. Glrx knockdowned C2C12 cells by siGlrx were transfected with ad human Glrx, which is resistant to siGlrx. Levels of HIF-1α, human, and mouse Glrx were analyzed by Western blotting. (*H*) Effect of HIF-1α knockdown on increment of mRNA levels of Vegfa by siGlrx. HIF-1α was knocked down by CRISPR/Cas9 in C2C12 cells. Then effect of siGlrx on mRNA expression of Vegfa was analyzed by qPCR. $^{\dagger}P < 0.05$, compared with respective vehicle-treated cells, $^{*}P < 0.05$.

Although we used global *Glrx* KO mice, a potential role of endogenous Glrx in myeloid cells in ischemic vascularization was excluded by bone marrow transplantation studies. Because Glrx is expressed ubiquitously, however, it remains unclear which type(s) of resident cells are important in the *Glrx* KO. Our *Glrx* KO mice data are consistent with endogenous Glrx orchestrating antiangiogenic actions through GSH adducts on HIF-1α and potentially other proteins. Therefore, down-regulation of Glrx itself can be a potential therapeutic target to promote ischemic limb revascularization.

In conclusion, GSH adducts on HIF-1α Cys^{520} induced by ischemia and Glrx deletion stabilize the protein and improves revascularization after hind limb ischemia in mice. Glrx ablation may be a therapeutic strategy to locally induce angiogenic genes in ischemic limbs.

Materials and Methods

Reagents. Cell culture reagents were obtained from Invitrogen. Reduced glutathione (G4251), oxidized glutathione (G4376), and 2-AAPA were from Sigma Aldrich. Anti–β-tubulin antibody (2128) and anti–hydroxy-HIF-1α antibody (3434) were from Cell Signaling, anti-GSH antibody was from Virogen (101-A-100), anti–HIF-1α polyclonal antibody was from Cayman (10006421), anti-VEGF antibody was from Santa Cruz Biotechnology (sc-152), anti-Flag antibody was from Sigma Aldrich (F7425), and anti-VHL antibody was from BD Pharmingen (556347). Human and mouse Glrx antibodies were custom ordered from Bethyl Laboratories. Human HIF-1α plasmid was from Sino Biological (HG11977-NH). Recombinant HIF-1α was from Abnova (H00003091-P01).

Cell Culture. C2C12 myoblast cells were grown in DMEM supplemented with 10% (vol/vol) FBS. For differentiation to myotubes, C2C12 cells were cultured in DMEM with 1% FBS for 5 d before experiments. Validated stealth siRNA oligonucleotides to Glrx were purchased from Invitrogen. Transfection of siRNA against Glrx (CCUACUGCAGAAAGACCCAAGAAAU, AUUUCUUGGGUCUUUCUGCAGUAGG) or nonsilencing control (CCUACGUAAAGCCAGGAACACAAAU, AUUUGUGUUCCUGGCUUUACGUAGG) to C2C12 cells was performed using Viromer Blue (VB-01LB; Lipocalyx) twice following the manufacturer's protocol before differentiation. For human Glrx overexpression in C2C12 cells, ad human Glrx (13) was transfected to undifferentiated C2C12 cells for 3 h. Then medium was changed to DMEM containing 1% FBS for differentiation 3 d after transfection cells were lysed and used for the following experiment. For GSSG ester treatment, medium was changed to DMEM without FBS, and these cells were treated with 50 μmol/L GSSG ester for 10 h. COS7 cells were seeded to 6-well plates and transfected with WT HIF-1α and C520S mutant HIF-1α (0.25 μg/well) using Lipofectamin 2000 (0.5 μL/well). These cells were treated with 20 μmol/L 2-AAPA for 3 h in serum-free DMEM 2 d after transfection. Adenoviral vector that expresses adenoviral tetracycline-responsive element–driven Glrx-conjugated GFP protein (Ad tet-Glrx) was a generous gift from Reto Asmis, University of Texas Health Science Center, San Antonio. Glrx overexpression was induced by using Ad tet-Glrx as described previously (19) by adding doxycycline (1 μg/mL) overnight. No human samples are used in this study. Work with human cells and plasmids was approved by the Boston University Medical Campus institutional biosafety committee.

HIF-1α Knockdown by CRISPR/Cas9. pSpCas9(BB)-2A-Puro (PX459) V2.0 plasmid used for generating a CRISPR-Cas9 endonuclease was a gift from Feng Zhang, Broad Institute, Massachusetts Institute of Technology, Cambridge, MA, obtained via Addgene (Addgene plasmid 62988). HIF-1a KO by CRISPR/Cas9 was performed as described previously with slight modifications (33). Insert oligonucleotides that include a guiding RNA sequence were designed as follows: for KO green monkey HIF-1α (COS7 cells), CACCGCGGGGACCGATTCACCATGG and AAACCCATGGTGAATCGGTCCCCGC; and for KO mouse HIF-1α (C2C12 cells), CACCGCACCCTAACAAGCCGGGGG, AACCCCCCGGCTTGTTAGGGTGC. After annealing, these oligonucleotides were inserted to the BbsI cloning site of PX459. These plasmids and unmodified PX459 plasmid were transfected to COS7 cells and C2C12 cells by using Lipofectamin 2000, respectively. Puromycin selection was performed after 1-d transfection for 2 d. After selection, cells were expanded and used for experiments.

Synthesis of Oxidized Glutathione Ethyl Ester. Oxidized glutathione was esterified using acetyl chloride to produce an oxidized glutathione glycine-*O*-monoethyl ester. Briefly, 1 mol/L acetyl chloride in ethanol was prepared by adding 1.8 mL acetyl chloride (Sigma Aldrich) to 25 mL ice cold anhydrous ethanol. After 15 min, 2.5 g oxidized glutathione was dissolved and incubated on a rotator for 2 h at room temperature. The progress of the reaction was followed by TLC. When at least 98% of the oxidized glutathione has disappeared (about 2 h), the mixture was cooled on ice, and 25 mL cold ethanol was added. The solution was adjusted to pH 6 with triethylamine to precipitate the oxidized glutathione mono ethylester. The product was dried, triturated

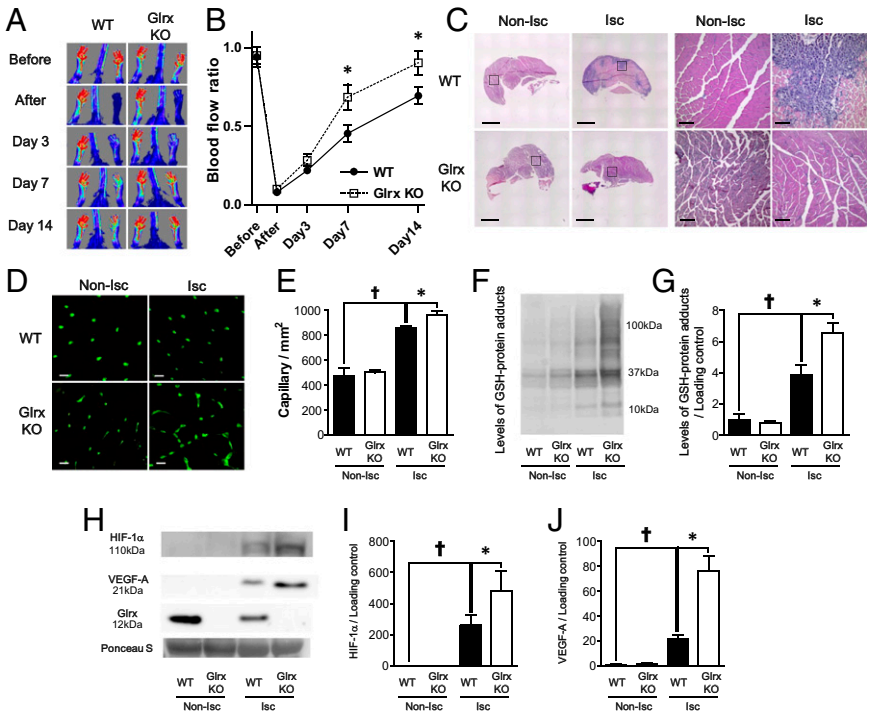

Fig. 3. Lack of Glrx improved ischemic revascularization after hind limb ischemia in mice. (*A* and *B*) Blood flow after hind limb ischemia was analyzed by LASER Doppler. (*A*) Representative images and (*B*) quantitative serial assessment ($n = 8$ each group). (*C*) Representative H&E staining of nonischemic (Non-Isc) and ischemic (Isc) gastrocnemius muscles of WT and *Glrx* KO mice. Squire area in low-power field images (*Left*) are shown by high-power images (*Right*). Black bar is 1 mm for low-power images and 100 μm for high-power field images. (*D* and *E*) Capillary density measurement in gastrocnemius muscles of WT and *Glrx* KO mice 7 d after HLI. Capillaries were stained with fluorescein-conjugated isolectin B4. (*D*) Representative images. (Scale bar, 50 μm.) (*E*) Graphical analysis ($n = 8$ each group). (*F* and *G*) Levels of protein GSH adducts in nonischemic (Non-Isc) and ischemic (Isc) gastrocnemius muscles of WT and *Glrx* KO mice were detected by anti-GSH antibody. (*F*) Representative blot and (*G*) densitometry analysis. (*H–J*) Western blot for HIF-1α, VEGF-A, and Glrx expression in muscles. (*H*) Representative blot, (*I*) densitometry analysis of HIF-1α, and (*J*) densitometry analysis of VEGF-A. Ponceau S staining showed equal loading of proteins and used as loading control to normalize protein expression ($n = 4$ each group). $^{\dagger}P < 0.05$ compared with nonischemic limbs; $^{*}P < 0.05$.

with dry t-butyl ether and ethanol, washed several times with t-butyl ether, and dried. The final product was dissolved in double distilled water and purified by Diaion HP20SS (Sigma Aldrich) column chromatography through stepwise elution with an increasing concentration of ethanol in water. The fraction containing oxidized glutathione glycine-*O*-monoethyl ester was lyophilized.

Mutagenesis Procedures. Plasmid that included human full-length cDNA of HIF-1α was used to construct Cys^{520} mutant HIF-1α. The Cys^{520}→Ser mutation was performed using the QuikChange II site-directed mutagenesis kit (200523; Agilent Technologies). Primers were designed as follows: GCCTAATAGTCCCAGTGAATATTCTTTTTATGTGGATAGTGATATGG and CCATATCACTATCCACATAAAAAGAATATTCACTGGGACTATTAGGC. The sequence of the construct was verified for DNA sequences (Tuft Medical Center, Sequencing Core). The Flag tag was added to the 5′ end by PCR to WT and C520S mutant HIF-1α. Primers were designed as follows, which include BamHI recognition and the Flag sequence for the 5′ end and the NotI recognition sequence for the 3′ end: forward, CGGGATCCATGGATTACAAGGATGACGACGATAAGGGTGGAGGCGGTAGCGAGGG; reverse, ATAGTTTAGCGGCCGCTTAGTTAACTTGATCCAAAGCTC. Then, the PCR product was inserted into pcDNA3.1, which cleaved with BamHI and NotI.

Co-IP Assay. HEK 293T cells in a 10-cm dish were transfected with 5 μg Flag WT HIF-1α, C520S mutant HIF-1α, or HA-VHL-pRc/CMV (34), which was a gift from William Kaelin, Dana-Farber Cancer Institute, Harvard Medical School, Boston, MA, via addgene (Addgene plasmid 19999) by using Lipofectamin 2000. WT or C520S mutant HIF-1α–transfected cells were lysed with 25 mmol/L Tris·HCl, 150 mmol/L NaCl, 10 mmol/L EDTA, 1% Triton, 1× protease, phosphatase inhibitor mixture (PI78441; Theromo Scientific), and lysate, which contains 500 μg protein treated with 100 mmol/L GSSG for 10 h. Then, desalting was performed with a Zeba column (89889; Thermo Fisher Scientific) to remove GSSG. These samples were mixed with 250 μg HA-VHL–transfected cell lysate, and Co IP was performed using a Pierce HA-Tag Magnetic IP/Co-IP kit (88838; Thermo Fisher Scientific). Detection of Flag–HIF-1α or HA-VHL was performed by immunoblotting by using anti-Flag antibody or anti-VHL antibody, respectively.

MS. HIF-1α recombinant protein (4 μg) was incubated with 25 mmol/L Tris·HCl, 30 mmol/L GSSG, and 70 mmol/L GSH, pH 8.0, for 12 h at room temperature and separated by SDS/PAGE. After electrophoresis, the gel was stained with Imperial protein stain (Thermo Fischer Scientific), and the band of HIF-1α was excised. The gel was washed with 25 mmol/L ammonium bicarbonate followed by acetonitrile three times. Digestion was performed with elastase at 37 °C for 18 h. MS analysis was performed by MS Bioworks (MSB-09). The gel digest was analyzed by nano LC/MS/MS with a Waters NanoAcquity HPLC system interfaced to a ThermoFisher Orbitrap Velos Pro. Peptides were loaded on a trapping column and eluted over a 75-μm analytical column at 350 nL/min; both columns were packed with Jupiter Proteo resin (Phenomenex). The MS was operated in data-dependent mode, with MS performed in the Orbitrap at 60,000 full width at half maximum resolution and MS/MS performed in the Velos. The 15 most abundant ions were selected for MS/MS.

RT-PCR. Total RNA was isolated from C2C12 cells using the Quick-RNA MicroPrep kit (R1050; Zymo Research). Then reverse transcription was performed to generate cDNA by using the High-Capacity RNA to cDNA kit (4387406; Thermo Fischer Scientific). Quantitative PCR was performed using gene-specific TaqMan primers (Invitrogen): 18S (Mm02601777_g1), Hif1α (Mm00468878_m1), Vegfa (Mm01281449_m1), Pdgfa (Mm01205760_m1), and Pdgfb (Mm00440677_m1), Fgf2(Mm00433207_m1). Expression levels were analyzed by comparative Ct (ΔΔCT) with StepOne real-time PCR software (Applied Biosystems).

Western Blots. Cells and tissue were lysed with 25 mmol/L Tris·HCl, 150 mmol/L NaCl, 10 mmol/L EDTA, 1% Triton, 1× protease, and a phosphatase inhibitor mixture (PI78441; Thermo Scientific). Samples were incubated with sample loading buffer (NP0007; Life Technologies) for 5 min at 95 °C. The protein assay was performed by Bio-Rad DC assay (500-0112; Bio-Rad), and an equal amount of proteins was separated by SDS/PAGE. For detection of GSH-protein adducts, proteins were analyzed in the nonreducing condition. After transfer, membranes were stained with Ponceau S, and images were obtained by scanning and then destained for the following experiments. After blocking with 5% (wt/vol) skim

milk in PBS with Tween 20 (0.1%) for 1 h, the membranes were incubated with the specific antibodies overnight at 4 °C, followed by the appropriate HRP-conjugated second antibody 1 h at room temperature. Images were visualized by LAS-4000 (GE Healthcare), and densitometry analysis was performed using ImageJ software (National Institutes of Health).

Histological Assessment. Mouse gastrocnemius muscles were obtained 1 wk after hind limb ischemia surgery and fixed with 4% (wt/vol) paraformaldehyde in PBS for 3 h and transferred to 30% (wt/vol) sucrose overnight. Then the samples were embedded in OCT compound, frozen, and serially sectioned (6 μm). Muscle sections were stained with H&E. Capillary density was quantified by staining with fluorescein-labeled GSL I-isolectin B4 (FL-1201; Vector Laboratory). Capillaries in the nonischemic and ischemic muscle were counted using ImageJ software, averaged from six images (200× magnification).

Biotin Switch Assay. Reversible oxidative cysteine modifications were analyzed by biotin switch assay. Differentiated C2C12 cells were treated with GSSG ester for 10 h. Then, cells were lysed with 25 mmol/L Tris·HCl, 150 mmol/L NaCl, 10 mmol/L EDTA, 1% Triton, and 100 mmol/L maleimide and incubated for 45 min at room temperature. After desalting with a Zeba column (89889; Thermo Fisher Scientific) to remove free maleimide, samples were reduced with 5 mmol/L DTT for 20 min in a conventional way or 30 mmol/L ascorbate for 1 h for the ascorbate-dependent biotin switch assay at room temperature. Samples were desalted again and labeled with 1 mmol/L *N*-(Biotinoyl)-*N*′-iodoacetyl ethylenediamine (BIAM) (90059; Biotium) for 1 h at room temperature. Free BIAM was removed using the desalting column three times. Then, 200 μg proteins was incubated with 200 μg streptavidin magnetic beads (S1420S; New England Bio Labs) for 1 h at 4 °C to pull-down biotin-labeled proteins. After washing three times with lysis buffer, proteins were eluted with 1× sample loading buffer and analyzed by Western blot.

Mice. Protocols for all mouse studies were approved by the Institutional Animal Care and Use Committee at Boston University. *Glrx* KO mice were originally generated by Y.-S. Ho (35) (Wayne State University, Detroit, MI) and were backcrossed to the C57BL/6 background in Yvonne Janssen-Heininger's laboratory (University of Vermont, Burlington, VT) and imported to Boston University. The mice were backcrossed (>10 crosses) onto C57BL/6J. Male *Glrx* KO mice and littermate WT controls were used in the present study. Mice are maintained in the laboratory animal science center at Boston University Medical Campus, and all procedures were approved by the Institutional Animal Care and Use Committee at Boston University.

Hind Limb Ischemia Model. Mice were anesthetized with ketamine (100 mg/kg) and xylazine (10 mg/kg) by i.p. injection. Hind limb ischemia was produced as described previously (13). Briefly, after ligation of the left femoral artery proximal to the superficial epigastric artery branch and anterior to the tibial artery branch, the segment of femoral artery between ligations was excised. Buprenorphine (0.5 mg/kg) was given before and after surgery for 3 d. Blood flow recovery was analyzed using LASER Döppler (Moor Instruments). After mice were anesthetized with ketamine (100 mg/kg) and xylazine (10 mg/kg) by i.p. injection, blood flow recovery was analyzed using LASER Döppler before and after surgery, as well as on days 3, 7, and 14. Blood flow was expressed as ratio of ischemic (left) to nonischemic (right).

Statistical Analysis. All group data are expressed as means ± SEM. Statistical analysis comparing two groups was carried out using the Student unpaired *t* test. Analysis of more than two groups was performed either by one-way ANOVA or two-way ANOVA, followed by the Tukey post hoc comparison test. Sequential measurements were analyzed by repeated measure one-way ANOVA. $P < 0.05$ was considered significant. All analysis was carried out using JMP software.

ACKNOWLEDGMENTS. We thank Xiang Weng for technical assistance. We thank Dr. Feng Zhang for providing PX459 V2.0 and Dr. William Kaelin for providing HA-VHL-pRc/CMV, respectively. This study was supported by National Institutes of Health Grants PO1 HL068758 and R37 HL104017 (to R.A.C.), RO1 HL133013 (to R.M.), and RO1 DK103750 (to M.M.B.); American Heart Association Grant 16GRNT27660006 (to M.M.B.); Robert Dawson Evans Scholar award from the Department of Medicine, Boston University (to R.A.C.); Sumitomo Life Welfare and Culture Foundation; and Mochida Memorial Foundation for Medical and Pharmaceutical Research (Y.W.).

1. Kris-Etherton PM, Lichtenstein AH, Howard BV, Steinberg D, Witztum JL; Nutrition Committee of the American Heart Association Council on Nutrition, Physical Activity, and Metabolism (2004) Antioxidant vitamin supplements and cardiovascular disease. *Circulation* 110(5):637–641.
2. Tojo T, et al. (2005) Role of gp91phox (Nox2)-containing NAD(P)H oxidase in angiogenesis in response to hindlimb ischemia. *Circulation* 111(18):2347–2355.
3. Urao N, et al. (2013) Critical role of endothelial hydrogen peroxide in post-ischemic neovascularization. *PLoS One* 8(3):e57618.
4. Craige SM, et al. (2011) NADPH oxidase 4 promotes endothelial angiogenesis through endothelial nitric oxide synthase activation. *Circulation* 124(6):731–740.
5. Ichihara S, et al. (2010) Ablation of the transcription factor Nrf2 promotes ischemia-induced neovascularization by enhancing the inflammatory response. *Arterioscler Thromb Vasc Biol* 30(8):1553–1561.
6. Burgoyne JR, Oka S, Ale-Agha N, Eaton P (2013) Hydrogen peroxide sensing and signaling by protein kinases in the cardiovascular system. *Antioxid Redox Signal* 18(9): 1042–1052.
7. Wang Y, Yang J, Yi J (2012) Redox sensing by proteins: Oxidative modifications on cysteines and the consequent events. *Antioxid Redox Signal* 16(7):649–657.
8. Li F, et al. (2007) Regulation of HIF-1alpha stability through S-nitrosylation. *Mol Cell* 26(1):63–74.
9. Klatt P, Lamas S (2000) Regulation of protein function by S-glutathiolation in response to oxidative and nitrosative stress. *Eur J Biochem* 267(16):4928–4944.
10. Wang Y-T, Piyankarage SC, Williams DL, Thatcher GRJ (2014) Proteomic profiling of nitrosative stress: Protein S-oxidation accompanies S-nitrosylation. *ACS Chem Biol* 9(3):821–830.
11. Chrestensen CA, Starke DW, Mieyal JJ (2000) Acute cadmium exposure inactivates thioltransferase (Glutaredoxin), inhibits intracellular reduction of protein-glutathionyl-mixed disulfides, and initiates apoptosis. *J Biol Chem* 275(34):26556–26565.
12. Mieyal JJ, Gallogly MM, Qanungo S, Sabens EA, Shelton MD (2008) Molecular mechanisms and clinical implications of reversible protein S-glutathionylation. *Antioxid Redox Signal* 10(11):1941–1988.
13. Murdoch CE, et al. (2014) Glutaredoxin-1 up-regulation induces soluble vascular endothelial growth factor receptor 1, attenuating post-ischemia limb revascularization. *J Biol Chem* 289(12):8633–8644.
14. Zhao Y, et al. (2009) Effects of glutathione reductase inhibition on cellular thiol redox state and related systems. *Arch Biochem Biophys* 485(1):56–62.
15. Clavreul N, et al. (2006) S-glutathiolation by peroxynitrite of p21ras at cysteine-118 mediates its direct activation and downstream signaling in endothelial cells. *FASEB J* 20(3):518–520.
16. Jaakkola P, et al. (2001) Targeting of HIF-alpha to the von Hippel-Lindau ubiquitylation complex by O2-regulated prolyl hydroxylation. *Science* 292(5516):468–472.
17. Ohh M, et al. (2000) Ubiquitination of hypoxia-inducible factor requires direct binding to the beta-domain of the von Hippel-Lindau protein. *Nat Cell Biol* 2(7):423–427.
18. Bachschmid MM, et al. (2010) Attenuated cardiovascular hypertrophy and oxidant generation in response to angiotensin II infusion in glutaredoxin-1 knockout mice. *Free Radic Biol Med* 49(7):1221–1229.
19. Ullevig S, et al. (2012) NADPH oxidase 4 mediates monocyte priming and accelerated chemotaxis induced by metabolic stress. *Arterioscler Thromb Vasc Biol* 32(2):415–426.
20. Barrett WC, et al. (1999) Regulation of PTP1B via glutathionylation of the active site cysteine 215. *Biochemistry* 38(20):6699–6705.
21. Adachi T, et al. (2004) S-Glutathiolation by peroxynitrite activates SERCA during arterial relaxation by nitric oxide. *Nat Med* 10(11):1200–1207.
22. Reynaert NL, et al. (2006) Dynamic redox control of NF-kappaB through glutaredoxin-regulated S-glutathionylation of inhibitory kappaB kinase β. *Proc Natl Acad Sci USA* 103(35):13086–13091.
23. Pineda-Molina E, et al. (2001) Glutathionylation of the p50 subunit of NF-kappaB: A mechanism for redox-induced inhibition of DNA binding. *Biochemistry* 40(47):14134–14142.
24. Shao D, et al. (2014) A redox-resistant sirtuin-1 mutant protects against hepatic metabolic and oxidant stress. *J Biol Chem* 289(11):7293–7306.
25. Bosch-Marce M, et al. (2007) Effects of aging and hypoxia-inducible factor-1 activity on angiogenic cell mobilization and recovery of perfusion after limb ischemia. *Circ Res* 101(12):1310–1318.
26. Semenza GL (2010) Vascular responses to hypoxia and ischemia. *Arterioscler Thromb Vasc Biol* 30(4):648–652.
27. Palmer LA, Gaston B, Johns RA (2000) Normoxic stabilization of hypoxia-inducible factor-1 expression and activity: Redox-dependent effect of nitrogen oxides. *Mol Pharmacol* 58(6):1197–1203.
28. Zee RS, et al. (2010) Redox regulation of sirtuin-1 by S-glutathiolation. *Antioxid Redox Signal* 13(7):1023–1032.
29. Huang B, Chen C (2006) An ascorbate-dependent artifact that interferes with the interpretation of the biotin switch assay. *Free Radic Biol Med* 41(4):562–567.
30. Chan PH (2001) Reactive oxygen radicals in signaling and damage in the ischemic brain. *J Cereb Blood Flow Metab* 21(1):2–14.
31. Tirziu D, et al. (2012) Endothelial nuclear factor-κB-dependent regulation of arteriogenesis and branching. *Circulation* 126(22):2589–2600.
32. Evangelista AM, Thompson MD, Bolotina VM, Tong X, Cohen RA (2012) Nox4- and Nox2-dependent oxidant production is required for VEGF-induced SERCA cysteine-674 S-glutathiolation and endothelial cell migration. *Free Radic Biol Med* 53(12): 2327–2334.
33. Ran FA, et al. (2013) Genome engineering using the CRISPR-Cas9 system. *Nat Protoc* 8(11):2281–2308.
34. Iliopoulos O, Kibel A, Gray S, Kaelin WG, Jr (1995) Tumour suppression by the human von Hippel-Lindau gene product. *Nat Med* 1(8):822–826.
35. Ho Y-S, et al. (2007) Targeted disruption of the glutaredoxin 1 gene does not sensitize adult mice to tissue injury induced by ischemia/reperfusion and hyperoxia. *Free Radic Biol Med* 43(9):1299–1312.